Theory of Fractal Growth

L. Pietronero,[1,2] A. Erzan,[1] and C. Evertsz[1]

[1]*Solid State Physics Laboratory, University of Groningen, Melkweg 1, 9718 EP Groningen, The Netherlands*

[2]*Dipartimento di Fisica, Università di Roma "La Sapienza," Piazzale Aldo Moro, 00185 Roma, Italy*

(Received 13 January 1988)

We introduce a new theoretical approach that clarifies the origin of fractal structures in irreversible growth models based on the Laplace equation and that provides a systematic method for the calculation of the fractal dimension. A specific application to the dielectric breakdown model (including therefore diffusion-limited aggregation) in two dimensions is presented. For fractal growth this new method appears to be more appropriate than the renormalization-group method.

PACS numbers: 64.60.Ak, 02.50.+s, 05.20.−y

The prototype fractal[1] growth models[2-4] are diffusion-limited aggregation (DLA)[5] and the more general dielectric breakdown model.[6,7] These models have been extensively studied in view of their intrinsic theoretical interest and because they are believed to capture the essential features of pattern formation in seemingly different physical phenomena.[3,4]

Most of the activity in this field has been based on computer simulations.[3,4,8] From the theoretical side there have been some interesting developments from the phenomenological point of view,[9] while the present applications of real-space renormalization-group methods to these problems are still unclear[10] and field-theory methods could provide definitive results only for the surface exponents of the two-dimensional Eden model.[11]

In this Letter we present a new theoretical approach to fractal growth that clarifies the origin of fractal structures in these models and provides a systematic approach to the calculation of the fractal dimension. A more complete description including a comparative discussion of this new method with respect to the renormalization-group method will be presented in a longer paper.[12]

Let us consider a frozen pattern (not modified by further growth) of dimension D grown with DLA[5] or the dielectric breakdown model[6] between two parallel lines as shown in Fig. 1. This geometry has the advantage of defining a growth direction and eliminates most of the lattice anisotropy complications. We now consider a process of box covering[1] for the $(D-1)$-dimensional set of points where the pattern is intersected by a line as shown in Fig. 1.

The elementary process by which a black box is subdivided into two leads to two possible configurations indicated as type 1 and type 2 (see bottom of Fig. 1). The corresponding probabilities in this process of fine graining are indicated by C_1 and C_2, respectively. Normalization requires that $C_1+C_2=1$. The average number of black subboxes that appear at the next level of fine graining from one black box is

$$\langle n\rangle=\sum_i n_i C_i = C_1+2C_2. \tag{1}$$

It is easy to show that the fractal dimension of the whole structure is related to the values of C_1 and C_2 by

$$D=1+\ln\langle n\rangle/\ln 2. \tag{2}$$

Given a certain level of fine graining, the distribution (C_1,C_2) corresponds therefore to the relative density of newly formed pairs (characterized by a dashed line) of types 1 and 2, respectively. However, this description is not complete because also large empty (white) segments appear. They correspond to the distribution of empty segments between two adjacent branches as indicated, for example, by λ_i and λ_j in Fig. 1. The probability of occurrence $P(\lambda)$ of a certain value of λ, can also be re-

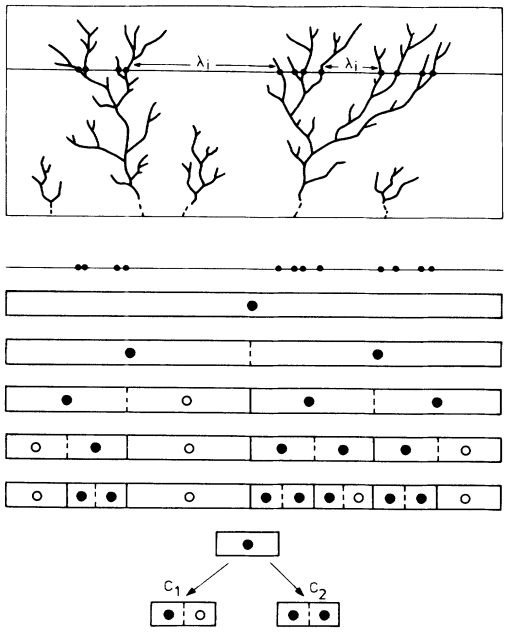

FIG. 1. Schematic picture of the process of box covering for the set of points given by the intersection of the fractal structure with a line. Dashed segments denote the first division of a cell. Bottom: elementary process of fine graining for a box (black) that contains some elements of the set.

lated to (C_1,C_2). If we define b as the lowest scale and $\lambda_n \neq b^n$ $(n=1,2,\ldots;\ \lambda_0 \sim 0)$, it can be shown by a nontrivial combinatorial analysis that[12]

$$P(\lambda_0 \sim 0) = C_2/(1+\tfrac{1}{2}C_1) \quad (n=0), \tag{3}$$

$$P(\lambda_n \sim b^n) = \frac{3}{2}\frac{C_1C_2}{(3-C_2)}(\tfrac{1}{2}+\tfrac{1}{2}C_1)^{(n-1)} \tag{4}$$

$$(n=1,2,3,\ldots).$$

Note that the λ distribution requires an analysis of all the steps of the fine-graining procedure.

In summary, all the properties of the system can be related to the distribution (C_1,C_2). Because of the scale invariance of the Laplace equation, the same distribution (C_1,C_2) is recovered if we consider the growth process at different scales. This, of course, provided that the system has reached an asymptotic distribution (C_1,C_2) independent of the initial conditions. The key point is, therefore, to find a systematic method to compute this distribution.

We now consider the conditional probability that, within a frozen region, a pair configuration (cell) of type 1 (or type 2) is followed, in the growth direction, by a cell of type 1 or 2, respectively. This gives rise to a *fixed-scale transformation* because the two cells considered are at the same scale. Note that the cells are defined as the basic ingredients of the fine- (or coarse-) graining procedure. In this respect we do not have to consider separately diagrams leading to two blank sites in the growth procedure. The processes involving such configurations in any combination with cells of type 1 or 2 are already included at a further level of fine graining in the processes that we consider in a similar way as shown in Fig. 1.

In order to compute this conditional probability, we consider growth conditional to the existence of a frozen cell of preassigned type. Therefore, growth is not considered within this initial cell. The growth process is then analyzed until the next cell in the growth direction becomes also statistically frozen. Figure 2 illustrates an example of this procedure. The initial frozen cell is of type 1 and it is denoted by a continuous line around it. The outer boundary condition can be located very close to the considered structure because we are only interested in relative probabilities within this structure. For the same reason we do not consider growth outside the column on top of the initial frozen cell. A nontrivial problem is the choice of lateral boundary conditions. For the moment, we adopt periodic boundary conditions with the period defined by the two dashed lines (Fig. 2). Later on, we are going to improve on this point. The relevant growth processes are indicated by the small arrows in Fig. 2. The first site to be occupied is necessarily the one above the occupied site of the initial cell; therefore, this is already included in the starting configuration [Fig. 2(a)]. Note that the growth direction in Fig. 2 should be interpreted as the local growth direction of the real structure. The analysis of further growth requires the knowledge of the potential field corresponding to this structure.[12] This defines the probabilities $p_{2,1}$ and $p_{1,1}=1-p_{2,1}$ for first-order processes. In a similar way, from the potential field corresponding to Fig. 2(b), one defines $p_{3,2}$ for second-order processes.

The probability that site 2 of Fig. 2(a) will be occupied *after infinite growth* gives the matrix $M_{1,2}$ corresponding to the conditional probability of having a frozen cell of type 1 followed by a frozen cell of type 2. This can be written as

$$M_{1,2}(\eta) = p_{2,1}(\eta) + [1-p_{2,1}(\eta)]p_{3,2}(\eta) + \cdots, \tag{5}$$

(where η has the usual meaning[6]) and, in principle, the series should be continued until the probability of occupation of site 2 in Fig. 2(a) is virtually negligible (freezing condition). It is important to note, however, that higher-order terms in this series correspond to configurations in which this site is strongly screened by growth that has occurred at other sites [see Fig. 2(b) in which the site 3 is the original site 2 of Fig. 2(a)]. This is because the penetration length for the potential given by the Laplace equation is of the size of the structure that one considers.[13] Such a fact is crucial because it allows rapid convergence of the series given by Eq. (5) to a number *different from 1* (except for the case $\eta \to 0$). *This is the key point for the formation of fractal struc-*

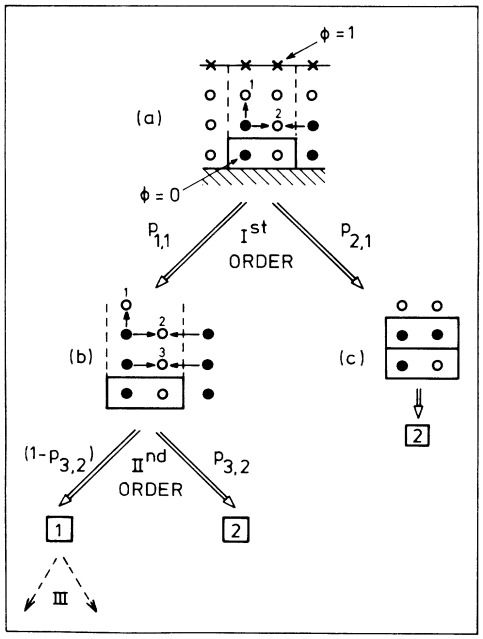

FIG. 2. Starting from a frozen cell of type 1 (encircled), we analyze the probability that asymptotically (after infinite growth) this is followed, in the growth direction, by a frozen box of type 1 or 2. Periodic boundary conditions are used with the period defined by the dashed lines.

tures. In fact, if Eq. (5) converges to a number smaller than 1, this implies that $M_{1,1}(\eta)=1-M_{1,2}(\eta)$ will be different from zero asymptotically. Therefore, there is a finite probability that growth will leave empty sites (holes) even asymptotically. In view of the scale invariance of the Laplace equation, this conclusion holds at any scale and therefore holes of all scales can be generated.

By considering the diagram that starts with a cell of type 2 (not shown), we can compute in a similar way the other two matrix elements $M_{2,1}(\eta)$ and $M_{2,2}(\eta)=1-M_{2,1}(\eta)$. These matrix elements completely define the fixed-scale transformation that leads to an iterative equation of transfer matrix type for (C_1,C_2):

$$\begin{bmatrix} C_1(\eta)^{(k+1)} \\ C_2(\eta)^{(k+1)} \end{bmatrix} = \begin{bmatrix} M_{1,1}(\eta) & M_{2,1}(\eta) \\ M_{1,2}(\eta) & M_{2,2}(\eta) \end{bmatrix} \begin{bmatrix} C_1(\eta)^{(k)} \\ C_2(\eta)^{(k)} \end{bmatrix}, \tag{6}$$

where k denotes the order of the iteration. The fixed point for the (C_1,C_2) distribution is given by

$$C_1^*(\eta)=\left[1+\frac{M_{1,2}(\eta)}{M_{2,1}(\eta)}\right]^{-1}. \tag{7}$$

The knowledge of (C_1^*,C_2^*), together with Eqs. (1) and (2), allows one to compute the fractal dimension D. For the case $\eta=1$ (DLA), we obtain $D=1.4747$ for the first-order processes, and $D=1.5418$ if we include also second-order. Inclusion of even higher orders shows convergency to about $D=1.55$.[12]

Such a value is rather low compared with the computer-simulations result $D\sim 1.70$.[8] This, however, was to be expected because the periodic boundary conditions (Fig. 2) imply that the structure is immediately followed by another branch and this produces a strong screening for the internal points. Now the λ distribution of Eqs. (3) and (4) provides the correct distribution of lengths between consecutive branches while the calculation that we have discussed corresponds only to the case $\lambda_0\sim 0$. This calls for a generalization of the theory in order to take into account the fluctuations of boundary conditions corresponding to the λ distribution. The matrix elements of the fixed-scale transformation are given in this case by the weighted averages for the different boundary conditions

$$\tilde{M}_{i,j}(\eta)=\sum_{n=0}^{\infty}P(\lambda_n)M_{i,j}(\eta;\lambda_n), \tag{8}$$

where $M_{i,j}(\eta;\lambda_n)$ corresponds to diagrams in which the next branch is at distance $\lambda_n=b^n$; $\lambda_0\sim 0$. In view of Eqs. (3) and (4) for $P(\lambda_n)$, the final matrix elements are now functions of all powers of (C_1,C_2) and the corresponding fixed-point condition,

$$C_1^*(\eta)=\left[1+\frac{\sum_{n=0}^{\infty}P(\lambda_n;C_1^*(\eta))M_{1,2}(\eta;\lambda_n)}{\sum_{n=0}^{\infty}P(\lambda_n;C_1^*(\eta))M_{2,1}(\eta;\lambda_n)}\right]^{-1}, \tag{9}$$

is a nonlinear equation of infinite order. From Eq. (4) we can see, however, that the effect of higher-order terms decays exponentially. As a simple approximation we may then assume that, as soon as λ_n is larger than or equal to b, the boundary condition is essentially open (λ_∞), while for $\lambda_0\sim 0$ it is closed as in the case treated before. This allows one to consider only two possibilities: closed configurations with probability $P_0=P(\lambda_0)=C_2/(1+C_1/2)$ and open configurations, corresponding to λ_∞, with probability $P_\infty=1-P(\lambda_0)$. The fixed-point equation [Eq. (9)] is then drastically simplified and its solution can be given in analytical form.[12]

The matrix elements corresponding to P_0 are those computed previously, while for the open boundary condition a new diagram analysis is needed. The details of this will be discussed elsewhere.[12] Here we only report the results of the λ_0-λ_∞ method for $\eta=1$: $D=1.6080$ for second order and $D=1.6406$ for third order. As expected, the self-consistent treatment of boundary-condition fluctuations has substantially improved our results.

Table I shows a summary of the values of $D(\eta)$ computed with the various methods discussed. The agreement with the computer simulations is very good for large values of η and less accurate for $\eta\to 0$. The origin of this effect becomes clear if we reconsider the freezing condition for the truncation of the series in Eq. (5). In the limit $\eta\to 0$ it is not enough to consider only a few terms in this series because the screening effect is essentially suppressed. In fact, by consideration of, for example, diagrams of the type of Figs. 2(a) and 2(b) (but, for simplicity, with open boundary conditions) it is easy to

TABLE I. Values of the fractal dimension as a function of the parameter η for the dielectric breakdown model in two dimensions computed with the various schemes of the theory discussed in this paper and compared with the results of computer simulations (Ref. 14). The case $\eta=1$ corresponds to DLA while $\eta=0$ gives one type of Eden model.

Present theory \ $\eta=$	0	0.5	1	2
λ_0; first order	1.7885	1.6465	1.4747	1.1885
λ_0; second order	1.8990	1.7515	1.5418	1.1997
λ_0-λ_∞; second order	1.8896	1.7549	1.6080	1.3956
λ_0-λ_∞; third order	1.9039	1.7830	1.6406	1.4190
Any λ; ∞ order	2	...	...	...
Computer simulations	2	1.92	1.70	1.43

show that for $\eta=0$ the probability that site 2 of Fig. 2(a) will never be occupied up to the Nth order process is

$$M_{1,1}(\eta=0)=\prod_{n=1}^{N}\frac{n}{n+1}$$
$$=\frac{1}{2}\frac{2}{3}\frac{3}{4}\cdots\frac{N-2}{N-1}\frac{N-1}{N}=\frac{1}{N}. \quad (10)$$

Therefore this point will be occupied with probability 1, leading to $D=2$, but only if processes of all orders are considered.

In summary, our new approach exploits the scale invariance of the Laplace equation that implies that the structure is self-similar under both growth and scale transformations. This allows one to introduce a fixed-scale transformation under growth (instead of coarse graining as in renormalization-group theory) that defines a functional equation for the fixed point of the distribution of basic diagrams used in the coarse-graining process. In addition, the analysis of the freezing condition for a given cell requires the study of an infinite number of processes that occur *outside* this cell. This is not in the spirit of the usual applications of renormalization-group theory[10] and it can be done much better with the fixed-scale transformation.

L. Pietronero is grateful to G. Parisi, L. Peliti, A. P. Siebesma, A. Vulpiani, and Y. C. Zhang for interesting discussions.

[1]B. B. Mandelbrot, *The Fractal Geometry of Nature* (Freeman, New York, 1982).

[2]*Kinetics of Aggregation and Gelation,* edited by F. Family and D. P. Landau (North-Holland, New York, 1984).

[3]H. E. Stanley and N. Ostrowsky, *On Growth and Form* (Martinus Nijhoff, Dordrecht, 1986).

[4]*Fractal in Physics,* edited by L. Pietronero and E. Tosatti (North-Holland, New York, 1986).

[5]T. A. Witten and L. M. Sander, Phys. Rev. Lett. **47**, 1400 (1981), and Phys. Rev. B **27**, 5686 (1983).

[6]L. Niemeyer, L. Pietronero, and H. J. Wiesmann, Phys. Rev. Lett. **52**, 1033 (1984).

[7]L. Pietronero and H. J. Wiesmann, J. Stat. Phys. **36**, 909 (1984).

[8]P. Meakin, Phys. Rev. A **27**, 1495 (1983). See also a recent review, in "Phase Transitions and Critical Phenomena," edited by C. Domb and J. Lebowitz (Academic, New York, to be published), Vol. 12.

[9]L. A. Turkevich and H. Scher, Phys. Rev. Lett. **55**, 1026 (1985); R. C. Ball, R. M. Brady, G. Rossi, and B. R. Thompson, Phys. Rev. Lett. **55**, 1406 (1985); T. C. Halsey, P. Meakin, and I. Procaccia, Phys. Rev. Lett. **56**, 854 (1986); C. Amitrano, A. Coniglio, and F. Di Liberto, Phys. Rev. Lett. **57**, 1016 (1986); R. C. Ball, Physica (Amsterdam) **140A**, 62 (1986).

[10]H. Gould, F. Family, and H. E. Stanley, Phys. Rev. Lett. **50**, 686 (1983); T. Nagatani, J. Phys. A **20**, L381 (1987); T. W. Burkhard and J. M. J. van Leeuwen, *Real Space Renormalization* (Springer-Verlag, Heidelberg, 1982).

[11]M. Kardar, G. Parisi, and Y. C. Zhang, Phys. Rev. Lett. **56**, 889 (1986); G. Parisi and Y. C. Zhang, J. Stat. Phys. **41**, 1 (1985).

[12]L. Pietronero, A. Erzan, and C. Evertsz, to be published.

[13]L. Pietronero, C. Evertsz, and H. J. Wiesmann, in Ref. 4, p. 159.

[14]The computer-simulations values of Table I are from H. J. Wiesmann and L. Pietronero, in Ref. 4, p. 151. However, they are also in agreement with the results of other authors. See Refs. 3, 4, and 8.